A COMPREHENSIVE APPROACH TO EFFICIENT CATALOGUING OF MANOEUVRABLE SATELLITES

Paula Díaz Morales [(1)], Daniel Gil Calvo [(2)], Arianna Rigo [(3)], Annalisa Mazzoleni [(4)]

[(1)] *Indra-Deimos, Ronda de Poniente 19 – 28760 Tres Cantos, Madrid (Spain), Email: pdmorales@indra.es*
[(2)] *Indra-Deimos, Ronda de Poniente 19 – 28760 Tres Cantos, Madrid (Spain), Email: dgilc@indra.es*
[(3)] *Indra-Deimos, Ronda de Poniente 19 – 28760 Tres Cantos, Madrid (Spain), Email: arigo@indra.es*
[(4)] *Indra-Deimos, Ronda de Poniente 19 – 28760 Tres Cantos, Madrid (Spain), Email: amazzoleni@indra.es*

ABSTRACT

This study addresses the challenges of cataloguing manoeuvrable satellites in the Geostationary Earth Orbit (GEO) region, focusing on detecting and estimating manoeuvres in quasi-real time without relying on external catalogues. The proposed three-step methodology uses optical sensor data and orbit determination techniques. First, the observed track is correlated with a known object. Next, potential manoeuvres are identified by comparing pre-manoeuvre propagated orbits with new observations, estimating the manoeuvre epoch, direction, and magnitude. Finally, a Batch Least Squares Orbit Determination refines the manoeuvre estimation. This approach enhances tracking accuracy, mitigating risks associated with unexpected trajectory changes and ensuring the safety of operational satellites in increasingly congested orbits. Leveraging Deimos' experience with GEO object cataloguing, this methodology offers a robust, autonomous solution for space situational awareness, improving the timely detection of manoeuvres and contributing to the long-term sustainability and security of space activities.

1 INTRODUCTION

The increasing congestion of the Geostationary Earth Orbit (GEO) region presents significant challenges for space situational awareness (SSA) and the maintenance of comprehensive satellite catalogues [2]. Among the numerous objects in GEO, manoeuvrable satellites introduce additional complexity due to their ability to perform unexpected trajectory changes. More than 500 operational satellites in GEO regularly execute manoeuvres, primarily for station-keeping and collision avoidance [6]. These manoeuvres affect orbit determination (OD) processes and can lead to miscorrelations or loss of track if not properly identified and catalogued.

1.1 Challenges in Post-Manoeuvre Tracking

The problem of accurately cataloguing manoeuvrable satellites in GEO stems from the need to track and characterize sudden changes in orbital parameters. Traditional cataloguing approaches assume that satellite orbits remain largely predictable over time, an assumption that fails in the presence of frequent manoeuvres. When processing post-manoeuvre tracks, three problematic scenarios may arise: (1) correct correlation with high residuals due to unmodeled trajectory changes, reducing the accuracy of computed orbits; (2) incorrect correlation, where a track is mistakenly associated with another object, potentially degrading the orbit estimates of both objects; and (3) no correlation, where the track fails to match any known object, leading to its classification as an unknown object. Addressing these issues is crucial for ensuring catalogue integrity and avoiding cascading errors in subsequent OD processes.

1.2 Background

The detection of satellite manoeuvres is a critical aspect of SSA, ensuring accurate orbit determination and collision avoidance in the increasingly congested GEO environment. Various algorithms and methodologies have been developed to tackle this challenge, each with distinct approaches and trade-offs.

One approach for manoeuvre detection in GEO satellites relies on publicly available Two-Line Element (TLE) datasets. A method was developed to filter raw orbit data, detect anomalies, and characterize manoeuvres using two approaches: the Manoeuvre Detection Method, which flags deviations exceeding a set threshold, and the Frequency Fit Method, which identifies regular manoeuvre cadences by minimizing residuals. This dual approach effectively distinguishes in-plane (IP) and out-of-plane (OOP) manoeuvres while identifying propulsion types [1].

Another investigation explored algorithms like the Extended Semi-analytic Kalman Filter (ESKF) and a hybrid method combining binary search and adaptive ESKF. The ESKF enhances linearity in orbital parameters through the Draper Semi-analytic Satellite Theory (DSST), improving detection accuracy. The hybrid algorithm achieved a 94% detection rate with an average detection lag of one day, balancing sensitivity and false positives [3].

Further advancements have focused on using Interactive

Proc. 9th European Conference on Space Debris, Bonn, Germany, 1–4 April 2025, published by the ESA Space Debris Office
Editors: S. Lemmens, T. Flohrer & F. Schmitz, (http://conference.sdo.esoc.esa.int, April 2025)

Multiple Models (IMM) and Unscented Kalman Filters (UKF) to improve detection robustness in scenarios with low observation density. Other approaches frame manoeuvre detection as an Optimal Control Problem (OCP), minimizing propellant usage to predict manoeuvre behaviour, and have been refined through multi-hypothesis tracking frameworks [5].

Recent efforts have explored the application of supervised machine learning techniques, particularly Convolutional Neural Networks (CNNs), to detect manoeuvres in GEO. One study developed a CNN trained on longitudinal shift manoeuvres using TLE data from the U.S. Space Command's space object catalogue [6]. The algorithm converts TLE data into geographic position histories (longitude, latitude, and altitude) and identifies anomalies through deviations from a satellite's nominal pattern of life. The study demonstrates that CNNs can successfully classify manoeuvre types such as longitudinal shifts, station-keeping adjustments, and unexpected drifts.

Another work expanded on this approach by introducing a refined labelling strategy for longitudinal shift manoeuvres. The study classified manoeuvres into components such as initiating or ending eastward/westward drift and employed a suite of CNN-based algorithms to enhance classification accuracy [7]. The results showed that manoeuvre detection using deep learning could achieve high recall rates but faced challenges in precision due to false positives.

A recent study presented at the 8th European Conference on Space Debris highlighted the prevalence of manoeuvrable satellites in the GEO regime, noting that more than 500 operational satellites perform manoeuvres every one or two weeks to maintain their designated orbital positions. This emphasizes the growing need for robust manoeuvre detection techniques to ensure accurate orbit determination and collision avoidance in the increasingly congested GEO environment [8].

Despite these advancements, challenges remain in achieving timely detection and accurate estimation without relying on external catalogues.

1.3 Main Contributions

This paper proposes a novel three-step methodology to enhance the cataloguing of manoeuvrable satellites in GEO using optical sensor data and OD techniques. The first step involves identifying the observed object to ensure correct correlation. The second step detects potential manoeuvres by comparing pre-manoeuvre propagated orbits with new observations, estimating the manoeuvre epoch, direction, and magnitude. Finally, a Batch Least Squares Orbit Determination refines the manoeuvre estimation. This approach operates in quasi-real time, addressing the limitations of previous methods by providing rapid and accurate manoeuvre characterization without external catalogue reliance.

1.4 Outline

The remainder of this paper is structured as follows: Section 2 details the equations underpinning the detection and estimation methodology. Section 3 presents the proposed methodology, describing the object identification, manoeuvre detection, and manoeuvre estimation steps. Section 4 discusses the results obtained for the GEO region, demonstrating the effectiveness of the approach. Finally, Section 5 concludes with a discussion of potential improvements and future work.

2 EQUATIONS

This section presents the derivation of key relationships between orbital parameters relevant to GEO manoeuvres. These provide the basis for the subsequent methodology implemented. Starting from well-known astrodynamics equations [4] we derive:

1. The relationship between declination and inclination, demonstrating that for small inclination changes in GEO orbits, the variation in declination closely approximates the variation in inclination.
2. The relationship between right ascension and semi-major axis, showing how variations in the semi-major axis influence right ascension drift over time.

2.1 Declination-Inclination Relationship

For GEO, the variation in declination can be used to approximate the variation in inclination during inclination change manoeuvres. Starting from well-known formulas in astrodynamics, we derive this relationship under the small inclination approximation.

The position vector in an Earth-Centred Inertial (ECI) frame is expressed in terms of right ascension (α) and declination (δ) [4]:

$$\vec{r} = \begin{bmatrix} r_I \\ r_J \\ r_K \end{bmatrix} = r \begin{bmatrix} \cos\delta \cos\alpha \\ \sin\delta \sin\alpha \\ \sin\delta \end{bmatrix} \quad (1)$$

where r is the magnitude of the position vector.

The satellite position in the orbital plane is given in the perifocal coordinate system (PQW frame):

$$\vec{r}_{PQW} = r \begin{bmatrix} \cos\nu \\ \sin\nu \\ 0 \end{bmatrix} \quad (2)$$

where ν is the true anomaly. Transforming from PQW to ECI requires a sequence of rotations:

$$\vec{r}_{ECI} = R_3(-\Omega)R_1(-i)R_3(-\omega)\vec{r}_{PQW} \quad (3)$$

Expanding this yields the ECI components, with the K-axis (OOP component) given by:

$$r_K = r \sin i \sin u \quad (4)$$

where $u = \omega + \nu$ is the argument of latitude.

Geocentric declination (DE or δ) is defined as the angle between the position vector and the equatorial plane:

$$\delta = \arcsin\left(\frac{r_K}{r}\right) = \arcsin(\sin i \sin u) \quad (5)$$

In GEO orbits, inclination $i \approx 0°$, allowing the small-angle approximation $\sin i \approx i$ (in radians):

$$\delta \approx i \sin u \quad (6)$$

As u varies between $-90°$ and $+90°$ over half an orbit, the maximum declination becomes:

$$\delta_{max} \approx i \quad (7)$$

Thus, for small inclinations:

$$\Delta\delta \approx \Delta i \quad (8)$$

The derivation of Eq. 8 shows that under the small inclination assumption, valid for GEO orbits, the change in geocentric declination closely approximates the change in inclination. Therefore, the declination difference can be used as an indicator for inclination changes in GEO inclination manoeuvres. The topocentric declination variation, as measured from the telescope location on Earth, can be assumed to be the same as the geocentric declination variation, due to the small declination variations and the GEO altitude.

2.2 Right Ascension - Semi-Major Axis Relationship

The variation of the semi-major axis (SMA or a) is related to changes in right ascension (RA or α) over time.

The mean motion is expressed as [4]:

$$n = \sqrt{\frac{\mu}{a^3}} \quad (9)$$

where μ is Earth's gravitational parameter. The right ascension rate is given by:

$$\frac{d\alpha}{dt} = \omega_{Earth} - n \quad (10)$$

For small changes in a, differentiating with respect to a gives:

$$\frac{d\alpha}{da} = \frac{3}{2}\sqrt{\frac{\mu}{a^5}} \quad (11)$$

Thus, a small variation Δa results in:

$$\Delta\alpha \approx \frac{3}{2}\sqrt{\frac{\mu}{a^5}}\,\Delta a\, T \quad (12)$$

This shows that the right ascension drifts due to semi-major axis variations, affecting satellite longitude.

3 PROPOSED METHODOLOGY

The proposed methodology consists of a three-step process aimed at efficiently detecting and estimating manoeuvres in quasi-real time, ensuring timely updates to satellite catalogues without external dependencies.

The process begins with constructing a catalogue of well-determined objects. Leveraging Deimos Space experience with GEO object cataloguing, regular optical observations are processed to establish accurate pre-manoeuvre orbits. This catalogue serves as the reference against which new observations are compared.

3.1 Object Identification

When new observations are received, the first step is identifying the object to ensure correct correlation. This process compares observed tracks with catalogued objects, identifying cases where residuals are high due to unmodeled trajectory changes, indicative of potential manoeuvres.

3.2 Manoeuvre Detection

Manoeuvre detection involves comparing angular measurements from the pre-manoeuvre propagated orbit with new observations. Variations in RA and DE provide insights into the nature of the manoeuvre using Eq.8 and Eq.12 to relates the variations in angles with the variation in the orbital elements, enabling a preliminary estimation of the manoeuvre epoch, direction, and magnitude. Depending on the observed changes, manoeuvres are categorized as:

- Increase in RA only: indicates an in-plane manoeuvre.
- Increase in DE only: suggests an out-of-plane manoeuvre causing an inclination change.
- Increase in both DE and RA: indicates an out-of-plane manoeuvre affecting both inclination and Right Ascension of the Ascending Node (RAAN) (a minor effect is also introduced in argument of perigee and eccentricity however is not treated in this paper).

This step is needed to get the pre-estimated manoeuvre and the interval epoch of the manoeuvre. The pre-estimation variables will be used as input in the Manoeuvre Estimation step.

3.3 Manoeuvre Estimation

Following detection, manoeuvre estimation refines the initial guess using a Batch Least Squares (BLS) OD algorithm. Pre- and post-manoeuvre tracks, along with pre-estimated manoeuvre parameters, are input into the BLS algorithm to accurately determine the manoeuvre epoch, direction, and magnitude as well as the manoeuvre-corrected satellite orbit.

For in-plane manoeuvres, the primary indicator is an increase in RA with minimal change in DE. High residuals confirm the occurrence of a manoeuvre, and the epoch is estimated by analysing angular changes. Semi-major axis is usually controlled to keep the longitude and manoeuvre time selected to keep the eccentricity vector under control.

Out-of-plane manoeuvres are characterized by noticeable changes in DE, with or without RA variations. Identifying the manoeuvre epoch involves tracking changes in the z-coordinate, pinpointing the ascending or descending node crossing. This information is fed into the BLS algorithm to refine the manoeuvre estimation. By combining these steps, the proposed methodology efficiently identifies and estimates manoeuvres, ensuring timely updates to satellite catalogues for the GEO region.

4 RESULTS FOR THE GEO REGION

The proposed methodology was applied to manoeuvre detection and estimation for an operational satellite in the GEO region, ASTRA5B. This satellite was selected due to its capability to perform both IP and OOP manoeuvres for station-keeping purposes.

4.1 Out-of-Plane Manoeuvre

The detection and estimation of an out-of-plane manoeuvre was performed using the declination-inclination relationship (Eq. 8) derived in Section 3.1.

4.1.1 Object Identification

The initial step in handling an out-of-plane manoeuvre is to identify the object under observation. After the manoeuvre has been executed, it is common to observe an increase in residuals when the orbit determination is performed. These high residuals can be an indicative of unmodeled trajectory changes resulting from the manoeuvre, which cannot be accounted for by the previous orbit parameters.

As shown in Fig. 1, the residuals exhibit a noticeable increase after the manoeuvre, confirming a significant deviation from the expected trajectory. When this occurs, we focus on determining whether the object has undergone an out-of-plane manoeuvre. This identification process involves comparing the observed angular changes with the predicted trajectory based on pre-manoeuvre data.

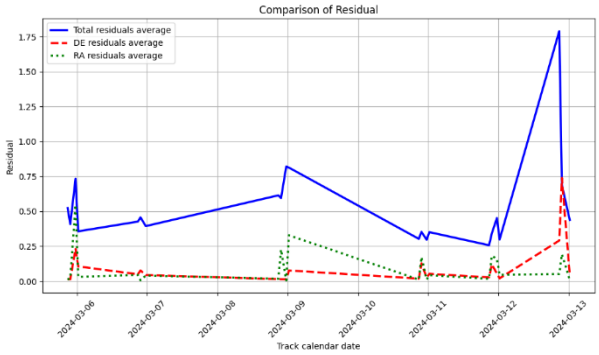

Figure 1. Residual analysis before and after a manoeuvre, showing significant deviations post-manoeuvre.

4.1.2 Manoeuvre Detection

The next step is to detect potential out-of-plane manoeuvres by comparing observed measurements with the pre-manoeuvre propagated orbit. Variations in angular differences between these datasets highlight discrepancies that help determine the nature and timing of the manoeuvre.

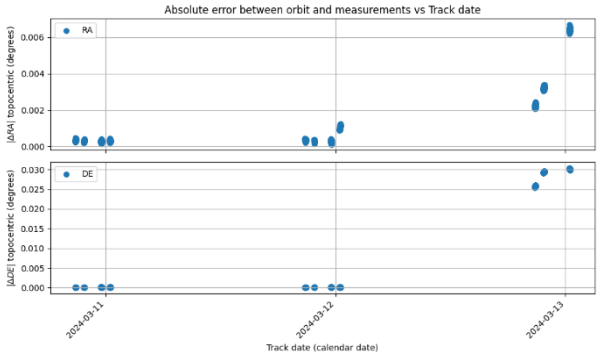

Figure 2. Declination and right ascension variation over time, indicating a potential inclination change.

The noticeable increase in both the right ascension (α) and declination (δ) angles in Fig. 2 suggests the occurrence of an out-of-plane manoeuvre, with a point of application that is not limited to the ascending or descending nodes. This change is further analysed to estimate the inclination change and its relation to the overall trajectory change.

The change in declination ($\Delta\delta$) in the topocentric frame, when compared to the geocentric frame, provides insights into the inclination change (Δi). The relationship between these angular changes is governed by the geometry of the orbit, allowing us to estimate the magnitude of the manoeuvre.

For the specific case of the out-of-plane manoeuvre, the following expression is used to estimate the magnitude of the pre-estimated velocity change [4][:

$$\left|\Delta\bar{V}_{pre-estimated}\right| = 2 \cdot V_1 \cdot \sin\frac{\Delta i}{2} \qquad (13)$$

where V_1 is the velocity module of the pre-manoeuvre orbit, and Δi represents the change in inclination.

The manoeuvre can be applied near either the ascending or descending node. The epoch at which the orbit crosses the orbital plane is determined by identifying changes in the sign of the z-coordinate.

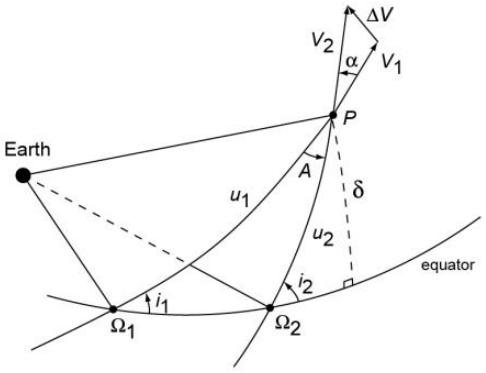

Figure 3. Geometric representation of an inclination change manoeuvre, showing velocity vectors before and after the manoeuvre, as well as the change in inclination and right ascension of the ascending node [9][.

Using the derived equations from the triangle geometry illustrated in Fig.3, we obtain the variations in right ascension of the ascending node and inclination change, which are plotted in Fig. 4. These variations depend on the argument of latitude of the pre-manoeuvre orbit u_1, showing periodic behavior as a function of orbital position.

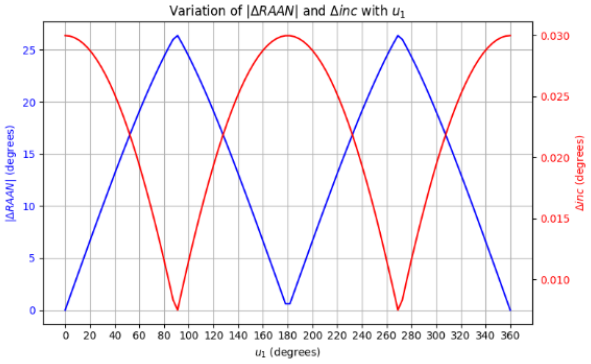

Figure 4. Variation of $|\Delta\Omega|$ (blue) and Δi (red) as a function of argument of latitude u_1, illustrating the periodic nature of the inclination change effect.

From Fig. 4, we observe that both $\Delta\Omega$ and Δi exhibit sinusoidal variation with respect to u_1. This implies that the effectiveness of an out-of-plane manoeuvre is highly dependent on the orbital position at which it is executed. Specifically, maximum changes in right ascension occur at different locations than maximum inclination changes, which is a key factor when designing orbital corrections.

We have 2 possibilities to apply the manoeuvre:

- Near ascending node ($u_1 \sim 0°$)

The interval epoch of the ascending node is determined using pre-manoeuvre orbital data. As the satellite crosses the orbital plane, its z-coordinate changes sign from negative to positive, indicating the ascending node. By examining the last observation before the manoeuvre and the first observation after, we identify two instances where this transition occurs, confirming the orbital plane crossing.

Tab. 1 presents the epochs and corresponding z-coordinates that illustrate this transition. The ascending node is precisely identified at the moment when the z-coordinate equals zero, which in this case occurs at 2024-03-12 16:25:41.793047.

Table 1. Visualization of ascending node crossing.

Epoch [calendar date]	Z coordinate [km]
2024-03-12T16:15:00	-2.597
2024-03-12T16:30:00	1.045
2024-03-12T16:25:41	0

Therefore, by adding a threshold of 0.05 days to the epoch of the passage through the ascending node, the time interval in which the manoeuvre could be executed is indicated in Eq.14.

$$2024\text{-}03\text{-}12T15{:}13{:}41 < t_{man\ AN} < 2024\text{-}03\text{-}12T17{:}37{:}41 \qquad (14)$$

Finally, if the manoeuvre is applied near the ascending node, the direction of the impulse will be as indicated in Eq.15

$$\Delta\bar{V}_{pre-estimated} = \left|\Delta\bar{V}_{pre-estimated}\right| \cdot \left(\cos\beta\ \hat{T} + \sin\beta\ \hat{N}\right) \qquad (15)$$

Where $\hat{T}$ and $\hat{N}$ are the tangential and normal direction of the orbit.

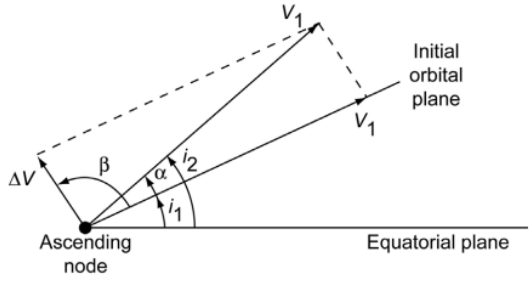

Figure 5. Geometric representation of the inclination change manoeuvre, illustrating velocity vectors before and after the manoeuvre, changes in inclination and RAAN, and the application of ΔV at the ascending node [9] [.

- Near descending node ($u_1 \sim 180°$)

Similarly, the descending node is identified when the satellite crosses the orbital plane in the opposite direction, with the z-coordinate changing from positive to negative. By analysing the pre- and post-manoeuvre observations, we determine the precise moment of this transition.

Table 2 presents the epochs and corresponding z-coordinates that illustrate this event. The descending node is identified at 2024-03-12T04:30:18, when the z-coordinate reaches zero.

Table 2. Visualization of descending node crossing.

Epoch [calendar date]	Z coordinate [km]
2024-03-12T04:30:00	7.481E-02
2024-03-12T04:45:00	-3.544
2024-03-12T04:30:18	0

Adding a threshold of 0.05 days to the epoch of the descending node, the interval epoch of the manoeuvre is as Eq.16.

$$2024\text{-}03\text{-}12T03{:}18{:}18 < t_{man\ DEs} < 2024\text{-}03\text{-}12T05{:}42{:}18 \quad (16)$$

Finally, the direction of the manoeuvre in the descending node is as indicated in Eq.17.

$$\Delta\bar{V}_{pre-estimated} = \left|\Delta V_{pre-estimated}\right| \cdot \left(\cos\beta\ \hat{T} - \sin\beta\ \hat{N}\right) \quad (17)$$

4.1.3 Manoeuvre Estimation

The manoeuvre estimation is perform using TRADE (Deimos Trajectory Determination Tool) in order to estimate the manoeuvre using the BLS orbit determination method.

Considering the two possible scenarios for the manoeuvre application, there are two cases in the manoeuvre estimation:

- Manoeuvre applied near ascending node:

  The pre-estimated parameters (input), obtained in the manoeuvre detection step, are shown in Tab. 3.

  Table 3. Pre-estimated out-of-plane manoeuvre (input parameters) in case the manoeuvre was applied in near the ascending node.

Reference frame	RTN	EME2000
ΔV_1 [km/s]	0	2.350E-06
ΔV_2 [km/s]	-3.760E-07	-3.237E-07
ΔV_3 [km/s]	1.520E-03	1.520E-03
Interval epoch [calendar date]	2024-03-12T15:13:41, 2024-03-12T17:37:41	

  The estimated manoeuvre are shown in Tab. 4.

  Table 4. Estimated out-of-plane manoeuvre (output results) in case the manoeuvre was applied in near the ascending node.

Reference frame	RTN	EME2000
ΔV_1 [km/s]	1.078E-04	4.104E-06
ΔV_2 [km/s]	-3.999E-06	-1.074E-04
ΔV_3 [km/s]	1.528E-03	1.758E-03
Manoeuvre epoch [calendar date]	2024-03-12 17:10:47.068997	

  Finally, he estimated orbit has been compared with the Special Perturbation (SP) methodology. As this is an out-of-plane manoeuvre applied near the ascending node, the most representative orbital element changes are the inclination and RAAN. Fig.6 and Fig.7 show the comparison of inclination and RAAN of both orbits respectively.

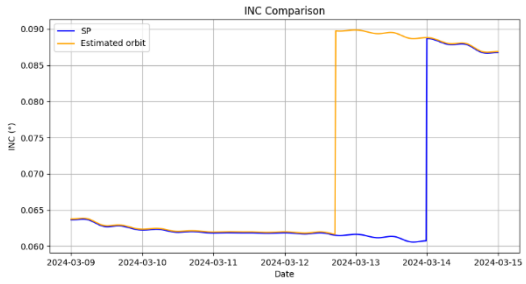

Figure 6. Change of inclination with time comparing the estimated orbit from the methodology and the corresponding SP.

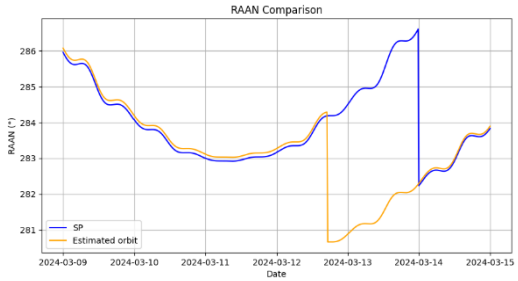

Figure 7. Change of RAAN with time comparing the estimated orbit from the methodology and the corresponding SP.

Fig.6 and Fig.7 indicate that the real manoeuvre was performed one day before that the date got from the SP orbit.

- Manoeuvre applied near descending node:

  In the case of the manoeuvre near the descending node, the pre-estimated parameters are detailed in Tab.5.

  Table 5. Pre-estimated out-of-plane manoeuvre (input parameters) in case the manoeuvre was applied in near the descending node.

Reference frame	RTN	EME2000
ΔV_1 [km/s]	0	-1.598E-06
ΔV_2 [km/s]	-3.760E-07	3.383E-07
ΔV_3 [km/s]	-1.520E-03	-1.520E-03
Interval epoch [calendar date]	2024-03-12T03:18:18, 2024-03-12T05:42:18	

In this case, the orbit determination method used could not find a converged solution therefore it is discarded that the manoeuvre is applied in the descending node.

4.2 In-plane manoeuvre

The detection and estimation of an in-plane manoeuvre were performed using the RA-semi-major axis relationship (Eq. 12) derived in Section 3.2.

4.2.1 Object Identification

The object identification process revealed a significant increase in the residuals, as shown in Fig. 8.

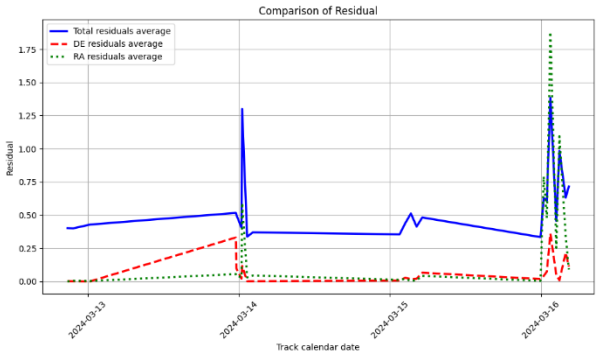

Figure 8. Residual analysis before and after a manoeuvre, showing significant deviations post-manoeuvre.

4.2.2 Manoeuvre Detection

The absolute errors between the orbit and measurements versus track date are plotted in Fig. 9. The increase in RA error further confirmed the presence of an IP manoeuvre.

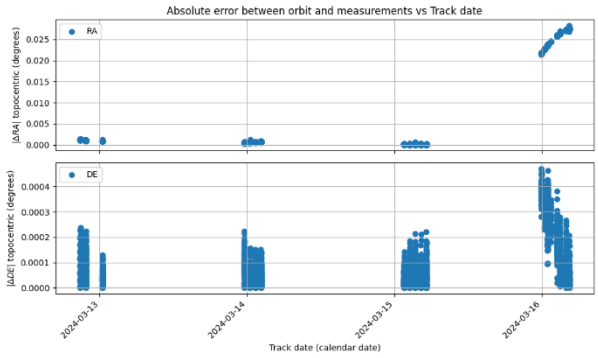

Figure 9. Absolute error between orbit and measurements versus track date, showing the increase in right ascension (RA) and declination (DE) errors, which further confirms the presence of an in-plane manoeuvre.

The equation for calculating the delta velocity in case of the in-plane manoeuvre is Eq.18 [4].

$$\left|\overline{\Delta V}_{pre-estimated}\right| = \sqrt{\left(\frac{2a_1 + \Delta a}{a_1 \cdot (a_1 + \Delta a)} - 2 \cdot \sqrt{\frac{1}{a_1 \cdot (a_1 + \Delta a)}}\right) \cdot \mu} \quad (18)$$

And the direction is tangential to the trajectory:

$$\Delta\bar{V}_{pre-estimated} = \left|\overline{\Delta V}_{pre-estimated}\right| \cdot \hat{T} \quad (19)$$

The manoeuvre application point was determined by analysing the sign of the semi-major axis variation, revealing a positive value ($\Delta a > 0$). Consequently, the maneuver was applied near the perigee. The perigee passage time was calculated using the following Eq.20 [4].

$$t_p = t_0 - \frac{M_0}{2\pi} \cdot T \quad (20)$$

Where M_0, t_0 are the mean anomaly and epoch of the pre-manoeuvre orbit in the reference time [deg, days], T is the orbit period [days] and t_p is the perigee passage time [days]. The results summarised in Tab. 6.

Table 6. Values of the variables used for calculating the perigee time passage in case of the in-plane manoeuvre.

Variable	Value
$M_0\ [deg]$	6.693
$t_0\ [days]$	8840.38909
$T\ [days]$	0.997
$T_p\ [days]$	8840.32410

Finally, the interval epoch where the manoeuvre can be performed is $t_p \pm$ threshold. Using a threshold of 0.1 days, the epoch interval is as indicated in Eq.21.

2024-03-15T05:22:42< t_{man} <2024-03-15T10:10:42 (21)

4.2.3 Manoeuvre Estimation

For the manoeuvre estimation, the pre-estimated manoeuvre parameters were used as inputs for the BLS OD, as detailed in Tab. 7. The output results from the estimation process are presented in Tab. 8, showing the refined manoeuvre parameters.

Table 7. Pre-estimated in-plane manoeuvre (input parameters) in case the manoeuvre.

Reference frame	RTN	EME2000
ΔV_1 [km/s]	0	2.474E-05
ΔV_2 [km/s]	7.112E-05	6.598E-05
ΔV_3 [km/s]	0	9.726E-07
Interval epoch [calendar date]	2024-03-15T05:22:42, 2024-03-15T10:10:42	

Table 8. Estimated in-plane manoeuvre (output results) after orbit determination.

Reference frame	RTN	EME2000
ΔV_1 [km/s]	2.474E-05	4.877E-05
ΔV_2 [km/s]	6.598E-05	5.087E-05
ΔV_3 [km/s]	9.726E-07	9.455E-07
Manoeuvre epoch [calendar date]	2024-03-15T09:23:27	

Finally, a comparison of the orbital elements of the orbit obtained applying the methodology with the ones obtained from the SP High-Accuracy catalogue has been made. The SMA changes are shown in Fig.10.

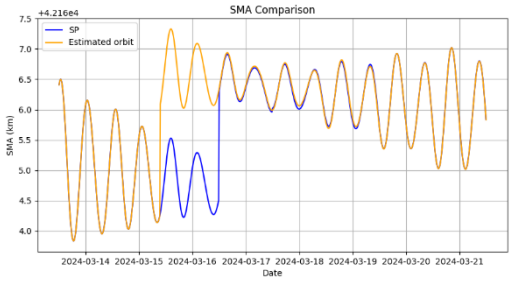

Figure 10. SMA change with time comparing the output orbit from TRADE and the corresponding SP.

Fig.10 shows with the methodology used, the manoeuvre can be detected in pseudo-real time and correct the orbit with no manoeuvre epochs delays.

5 CONCLUSIONS

The proposed methodology demonstrated a robust capability to detect and estimate satellite manoeuvres in the GEO region, focusing on both in-plane and out-of-plane manoeuvres. The stepwise process effectively identified objects, detected manoeuvre signatures, determined the manoeuvre direction, application points and magnitude, and refined manoeuvre parameters through a Batch Least Squares Orbit Determination process.

The key strength of this methodology lies in its ability to detect and estimate manoeuvres in quasi-real time without relying on external catalogues. This autonomous capability enhances the responsiveness and accuracy of the cataloguing process.

The results obtained for ASTRA5B validated the method accuracy and reliability. The ability to distinguish between different manoeuvre types using RA and DE variations allowed for a precise determination of manoeuvre epochs and characteristics. In particular, the analysis of orbital plane crossings and semi-major axis variations provided key insights into manoeuvre application points.

This methodology enhances space situational awareness by ensuring timely updates to orbital parameters, enabling a more effective and autonomous approach to catalogue maintenance. Future work could expand this method to a larger set of GEO satellites and incorporate additional sensor data to further improve detection accuracy and robustness.

6 REFERENCES

[1] Decoto, J., & Loerch, P. (2015, September). Technique for GEO RSO station keeping characterization and maneuver detection. In *Advanced Maui Optical and Space Surveillance Technologies Conference* (p. 42).

[2] ESA Space Debris Office (2024, July). ESA's Annual Space Environment Report, ESOC Darmstadt, Germany.

[3] Folcik, Z. J., Cefola, P. J., & Abbot, R. I. (2008). Geo maneuver detection for space situational awareness. *Adv. Astronaut. Sci*, *129*, 523-550.

[4] Vallado, D. A. (2013). Fundamentals of astrodynamics and applications (Fourth Edition). *Space Technology Library*, Microcosm Press, Hawthorne, CA.

[5] Porcelli, L., Pastor, A., Cano, A., Escribano, G., Sanjurjo-Rivo, M., Escobar, D., & Di Lizia, P. (2022). Satellite maneuver detection and estimation with radar survey observations. *Acta Astronautica*, 201, 274-287.

[6] Roberts, T. G., & Linares, R. (2020, October). Satellite repositioning maneuver detection in geosynchronous orbit using two-line element (TLE) data. In *71st International Astronautical Congress* (Vol. 10).

[7] Roberts, T. G., & Linares, R. (2021, September). Geosynchronous satellite maneuver classification via supervised machine learning. In *Advanced Maui Optical and Space Surveillance Technologies Conference*.

[8] Pastor, A., Escribano, G., Cano, A., Sanjurjo-Rivo, M., Perez, C., Urdampilleta, I., & Escobar, D. (2021, April). Manoeuvre detection and estimation based on sensor and orbital data. In *Proc. 8th European Conference on Space Debris, Darmstadt*.

[9] Wakker, Karel F. "Fundamentals of astrodynamics." *TU Delft Repository, Delft* (2015).